Original Paper

Cellular Physiology and Biochemistry

Cell Physiol Biochem 2011;28:103-114

Accepted: July 25, 2011

Ischemia Induces Closure of Gap Junctional Channels and Opening of Hemichannels in Heart-derived Cells and Tissue

David Johansen[1,2], Véronique Cruciani[2,4], Rune Sundset[1,3], Kirsti Ytrehus[1] and Svein-Ole Mikalsen[2,5]

[1]Cardiovascular Research Group, Department of Medical Biology, Faculty of Health Sciences, University of Tromsø, Tromsø, [2] Department of Cancer Prevention, Institute for Cancer Research, Oslo University Hospital, Oslo, [3]Section of Nuclear Medicine, University Hospital North Norway, Tromsø, [4]Present address: Affitech AS, Oslo Research Park, Oslo, [5]Present address: Faculty of Science and Technology, University of the Faroe Islands, Torshavn

Key Words

Hemichannels • Connexin 43• Pannexin 1 • Gap junction • Dithionite • Ischemia-reperfusion • Heart • Fibroblasts

Abstract

Aim: Gap junction intercellular communication (GJIC) and hemichannel permeability may have important roles during an ischemic insult. Our aim was to evaluate the effect of ischemia on gap junction channels and hemichannels. Methods: We used neonatal rat heart myofibroblasts and simulated ischemia with a HEPES buffer with high potassium, low pH, absence of glucose, and oxygen tension was reduced by dithionite. Microinjection, western blot, immunofluorescence, cell viability and dye uptake were used to evaluate the effects induced by dithionite. Isolated perfused rat hearts were used to analyse infarct size. Results: Short period with simulated ischemia reduced the ability to transfer a dye between neighbouring cells, which indicated reduced GJIC. Prolonged exposure to simulated ischemia caused opening of hemichannels, and cell death was apparent while gap junction channels remained closed. Connexin 43 became partially dephosphorylated and the total amount decreased during simulated ischemia. We were not able to detect the alternative hemichannel-forming protein, Pannexin 1, in these cells. The potential importance of Connexin 43 or Pannexin 1 hemichannels in ischemia-induced infarct in the intact heart was studied by perfusion of the heart in the presence of peptides that block one or the other type of hemichannels. The connexin-derived peptide, Gap26, significantly reduced the infract/risk zone ratio (control 48.7±4.2% and Gap26 19.4±4.1%, $p<0.001$), while the pannexin-derived peptide, ^{10}Panx1, did not change infarct/risk ratio. Conclusion: Connexin 43 is most likely responsible for both closure of gap junction channels and opening of hemichannels during simulated ischemia in neonatal rat heart myofibroblasts. Opening of connexin 43 hemichannels during ischemia-reperfusion seems to be an important mechanism for ischemia-reperfusion injury in the heart. By preventing the opening of these channels during early ischemia-reperfusion the infarct size becomes significantly reduced.

KARGER

Fax +41 61 306 12 34
E-Mail karger@karger.ch
www.karger.com

1015-8987/11/0281-0103$38.00/0

Accessible online at:
www.karger.com/cpb

David Johansen
Cardiovascular Research Group, Faculty of Health Sciences,
University of Tromsø, 9037 Tromsø (Norway)
Tel. +47-911 38076, Fax +47-776 45440
E-Mail david.johansen@uit.no

Introduction

Gap junctions are specialized membrane areas with structured aggregates of connexin proteins forming intercellular channels connecting the cytoplasms of two adjacent cells. In many tissues and cells, Connexin 43 (Cx43) is the predominant protein forming gap junction channels. Under resting conditions, gap junction channels are in an open state while hemichannels are predominantly in a closed state, and their gating is regulated, among other factors, by the phosphorylation status of the connexins [1]. The presence of non-junctional hemichannels located to the cell membranes has also been proposed [1].

Due to the widespread occurrence of atherosclerosis, ischemic injury is a common cause of organ dysfunction in humans, with the heart as an important victim. Ischemia results in accumulation of metabolites in the extracellular compartment in combination with reduced oxygen supply. Anaerobic metabolism and lack of flow cause severe intra- and extracellular acidosis. The loss of high-energy phosphate compounds leads to failure of membrane-based ion pumps resulting in increase in extracellular potassium [2]. We have previously shown that neonatal cardiac fibroblasts suffer time-dependent viability loss as a consequence of ischemia-like culture conditions [3]. These cells also respond to cardioprotective strategies in the same way as cardiomyocytes [3, 4].

There might be differences in the regulation of Cx43 hemichannels and gap junction channels during ischemia. Whereas metabolic inhibition opens Cx43 hemichannels [5], ischemia induces closure of gap junction channels, both when determined electrophysiologically [6] or by transfer of gap junction-permeable dyes [3, 7]. Increased cytosolic Ca^{2+} concentration, reduced ATP concentration, changes in phosphorylation of Cx43, and acidification, all occurring during ischemia, close gap junction channels [8], whereas a decrease in extracellular Ca^{2+} concentration or changes in phosphorylation have been described to open Cx43 hemichannels [1].

Hawat et al. [9] showed that Cx43 mimetic peptide Gap26 given during ischemia and reperfusion protected the heart against ischemia-reperfusion injury, and that this protection was due to inhibition of opening of Cx43 hemichannels.

More recently, another group of channel proteins, the pannexins, were discovered. Although there are structural similarities between connexins and pannexins, they appear to be two evolutionary distinct families [10]. In humans and other mammals there are three pannexins; 1, 2 and 3, where Pannexin 1 (Panx1) in particular forms hemichannels [11]. Thompson et al. [12] showed that ischemia opens neuronal Panx1 hemichannels. Panx1 is also widely expressed in the body [13], making it a potential candidate for hemichannel activities found in different cells and organs. Karpuk et al. [14] showed that Panx1 mimetic peptide ^{10}Panx1 can block Panx1 hemichannels during inflammation in astrocytes.

The first aim of this study was to correlate the time course of ischemia induced gap junction closure and phosphorylation pattern of Cx43. Since Cx43 exists both in gap junctions and in hemichannels the second aim was to test hemichannel opening in ischemia using cell cultures subjected to simulated ischemia and isolated hearts subjected to regional ischemia in order to determine hemichannel subtype and the role of these channels in cell death.

Materials and Methods

Animals

Adult female pregnant and non-pregnant Wistar rats (250-300g), from Charles River (Sulzfeld, Germany) were used in this study. They were treated according to the Guidelines on accommodation and care of laboratory animals by: The European Convention for the protection of vertebrate animals used for experimental and other scientific purposes (Council of Europe No. 123, Strasbourg 1985). The Norwegian Committee on Ethics in Animal Experimentation approved all procedures. Before heart harvesting rats were anticoagulated by heparin (200 IU per animal) and anesthetized with sodium pentobarbital (100 mg kg^{-1}) via intraperitoneal administration.

Chemicals and antibodies

Sodium dithionite (NaO_2SSO_2Na) was bought from Sigma (St. Louis, MO). Three anti-Cx43 antibodies were used. The rabbit polyclonal anti-Cx43 was from Sigma (C6219). This antibody recognizes an epitope in the extreme C-terminal tail of Cx43, and it is not affected by phosphorylations, and thus can recognize all phosphovariants of Cx43. The mouse monoclonal antibody 13-8300 was from Zymed (Carlsbad, CA). This antibody was first reported to recognize only the nonphosphorylated version of Cx43 [15], but was later shown also to recognize some phoshorylated versions of Cx43 [16]. The antibody binds to a serine-rich epitope (positions 364-373), and according to the supplier serine in position 368 must be nonphosphorylated for recognition to occur. The rabbit polyclonal phosphospecific anti-Cx43 antibody was from Chemicon (AB3841; Temecula, CA). According to the supplier, this antibody recognizes Cx43 when serine in position 368 is phosphorylated. For simplicity, the three antibodies will be called anti-Cx43 (C6219 from Sigma), anti-NP (13-8300 from Zymed) and anti-pS368 (AB3841 from Chemicon). Two anti-

Panx1 antibodies were used. Rabbit polyclonal anti-Panx1 was from Millipore (AB9886; Billerica, MA) and goat polyclonal anti-Panx1 from Santa Cruz (sc-49695; Santa Cruz, CA). A monoclonal anti-β-actin antibody (Sigma) was used for loading control.

Cell cultures and incubation in modified HEPES buffer

Rat neonatal fibroblasts were isolated from the hearts of 1-2 day old pups by enzymatic dissociating as previous described [3, 17]. Mass cultures were grown in Dulbecco's Modified Eagle's Medium supplemented with glutamine and 10% fetal calf serum (Invitrogen) in a humid 5% CO_2 atmosphere at 37 °C. Cells were maintained in culture until confluent.

To mimic ischemic conditions a HEPES buffer with elevated K^+, lowered pH and reduced oxygen content was used. The modified HEPES buffer was freshly made for every experiment and contained (in mM): 128 NaCl, 15.6 KCl, 0.5 $MgCl_2$, 0.9 $CaCl_2$, 20 HEPES, 20 lactate plus varying amounts of the oxygen scavenger dithionite (0-2.5 mM). After addition of dithionite in the given concentrations, pH was adjusted to 6.2 by addition of predetermined amounts of 0.2 M KOH, and immediately added to the cells as described below. A blood gas analyzer (Rapidlab 860, Chiron Diagnostics, Essex, UK) was used to measure oxygen tension in the modified HEPES buffer. Oxygen tension was measured at time 0, 15 min, 30 min, 60 min and 90 min in three separate experiments (Fig. 1).

The experiments were performed two days after seeding using nearly confluent cell monolayers. The growth medium was removed, and the cells rinsed twice with modified HEPES buffer containing the relevant concentration of freshly added dithionite (0, 0.25, 0.75 or 2.5 mM), before adding the buffer for a third time and leaving the cells at 37 °C in a humid atmosphere for 15, 30, 60, 90 or 120 min. The cells were then assayed as described below.

Cell death/survival was measured by the CellTiter AQ_{ueous} One Solution Cell Proliferation Assay (Promega; Madison, WI) as described by the supplier. The assay measures the formation of a formazan product in the presence of dehydrogenases and NADH [2]. Cells were seeded in 96 well plates (15,000 cells/well), and they were cultured for 48 h before use. The exposure to modified HEPES buffer was done as described above. At the end of the exposure period, the cells were gently washed twice in PBS before adding 100 µl DMEM (without serum) and 20 µl CellTiter solution, followed by 2 h incubation at 37 °C in a humid 5% CO_2 atmosphere. The medium (100 µl) was then transferred to another 96 well plate, and absorbance read at 492 nm. Cells that had not received any modified HEPES buffer indicated the relative cell viability of 1. The absorbance in wells without cells, but with medium (without serum) and CellTiter solution, was subtracted from all the other measurements. The data are presented as relative cell viability, and the experiment was done five times.

Dye transfer and hemichannel opening

Gap junction intercellular communication (GJIC) was assessed by microinjection of Lucifer Yellow (LY; 10% solution in water; Sigma) into single cells. Five minutes after injection, the cells were fixed in 4% formaldehyde in phosphate-buffered saline (PBS), and the number of dye-containing cells was counted.

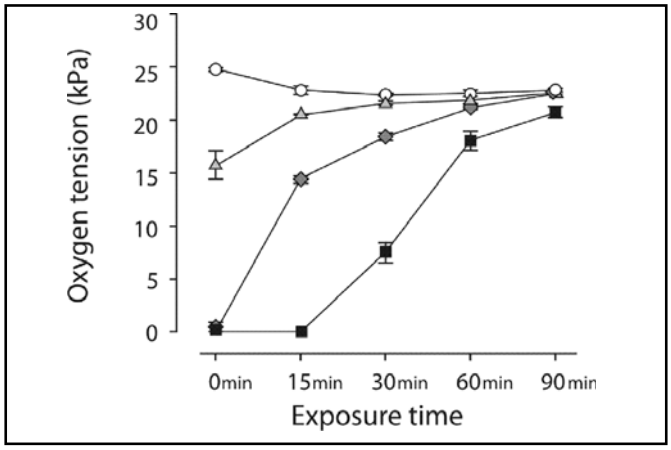

Fig. 1. Oxygen tension in modified HEPES buffer with different concentrations of dithionite over time. Modified HEPES buffer without dithionite (open circle), and with 0.25 mM (grey triangle), with 0.75 mM (grey diamond) and with 2.5 mM dithionite (filled square).

Hemichannel opening was assayed by adding LY to the modified HEPES buffer during the last 2 minutes of incubation. One ml buffer was transferred from the dish into a tube, and 10 µl of 10% LY was added to the tube followed by mixing. The remaining buffer was removed from the dish, and the LY-containing buffer was gently added to the dish. After 2 min of incubation, the dishes were gently rinsed twice in PBS before fixation in 4% formaldehyde. After 30 min, the cells were incubated for 5 min in 0.1% Triton X-100 in PBS for permeabilization, followed by 30 min incubation with 5 nM DAPI in PBS. The dishes were then rinsed three times in PBS before five randomly selected areas in each dish were photographed to reveal LY and DAPI. The number of nuclei stained by DAPI was taken as the total number of cells. LY uptake in endosomes could be seen as small dots, and was easily distinguished from uptake of LY through hemichannels, where the dye was uniformly spread out in the whole cell. The experiments have been done four times under identical conditions.

Western blotting

Cells were treated as described above. Samples were prepared by scraping the cells into electrophoresis sample buffer, followed by sonication. The samples were run on 7.5% polyacrylamide gels, and blotted onto nitrocellulose membranes. The different conditions have been examined at least three times, although all conditions have not been examined in every experiment.

Connexin 43

The membranes were blocked in 2% skimmed milk in Tris-buffered saline (TBS) for 1 h for anti-Cx43 and anti-NP, or in 0.1% Tween-20 in TBS (TBS-T) for anti-pS368. The membranes were probed with antibodies diluted in 0.4 % skimmed milk or 0.025% Tween-20 in TBS (1000-, 500-, 500 and 1000-fold dilutions

for anti-Cx43, anti-pS368, anti-NP and anti-β-actin, respectively) for 1 h, rinsed three times in TBS-T, before incubation with the relevant HRP-conjugated secondary antibodies (BioRad; Hercules, CA; 50,000 fold dilution in 0.4% skimmed milk or TBS-T) for 1 h. The antibodies were detected by chemiluminescence (Pierce; Rockford, IL).

Pannexin 1

After blocking for 1 h in 5% skimmed milk in TBS-T, the membrane was probed overnight at 4°C with anti-Panx1 (1:2000, Millipore) or anti-Panx1 (1:1000, Santa Cruz) in 3% skimmed milk in TBS-T. Following washing in TBS-T, the membrane was probed for 1 h at room temperature with HRP-conjugated anti-rabbit antibody (1:2000, CST) in 3% blocking buffer. After washing in TBS-T, Panx1 was visualized by chemiluminescence (Millipore).

Immunofluorescence

The cells were fixed in 4% formaldehyde in TBS for 30 min, before 5 min permeabilization in 0.1% Triton X-100 in TBS. The cells were blocked in bovine serum albumin (10 mg/ml in TBS) for 1 h. Anti-Cx43 (1:500), anti-pS368 (1:100) or anti-NP (1:100) were diluted in blocking solution and incubated for 1 h. After washing three times in TBS, the cells were incubated in anti-rabbit or anti-mouse secondary antibodies conjugated to Alexa488 (Molecular Probes; 1:1000 dilution in blocking solution) for 1 h. The samples were rinsed five times in TBS before mounting in Mowiol mounting medium.

Isolated perfused rat heart, infarct size measurements

Hearts from adult female Wistar rats were isolated and perfused in Langendorff mode [18]. Coronary flow rate (ml/min) was measured by timed collection of the coronary effluent and left ventricular pressure measured by the aid of an intraventricular balloon connected to a pressure transducer. All hearts were subjected to regional ischemia for 30 min, followed by 120 min reperfusion. Infarct measurements were performed using triphenyltetrazolium chloride (TTC) staining in combination with Evans blue for ischemic risk zone size determination as described elsewhere [18]. Necrotic tissue remained unstained while non-infarcted tissue was stained red by TTC. Stained x 2 mm thick sections were digitally analysed by ImageJ (ImageJ 1.44m, USA). Volumes were calculated as area x 2 mm, and infarct size was expressed as the percentage of infarct tissue volume within the ischemic risk zone volume. Hearts were excluded from further study if they failed to produce a left ventricular developed pressure greater than 60 mmHg during stabilisation, or they had a coronary flow rate outside the range 8-18 ml/min.

Hearts were divided into three groups: (i) Controls (n=6) were subjected to 25 min stabilisation followed by 30 min of regional ischemia and 120 min reperfusion. (ii) The second group received 0.5 μM Gap26, a Cx43 mimetic peptide (Anaspec, CA) (n=6), which was added from the last 2 minutes of ischemia to 10 min into reperfusion. (iii) The third group received 0.5 μM ^{10}Panx1, a Panx1 mimetic peptide (Anaspec, CA) (n=4), which was added from the last 2 minutes of ischemia to 10 min into reperfusion.

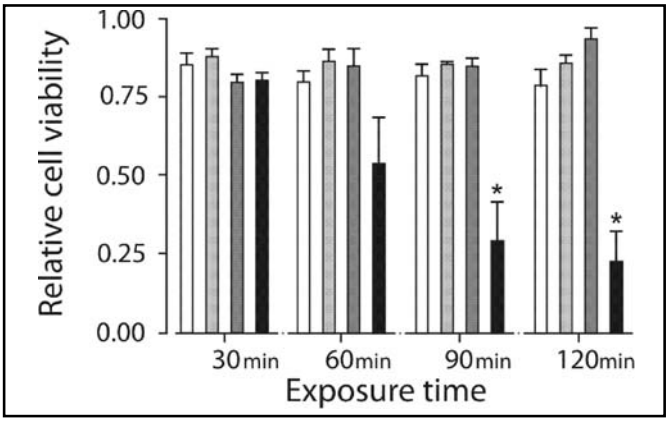

Fig. 2. Cell toxicity after exposure to modified HEPES buffer with/without dithionite. The cells were gently rinsed twice in PBS, and 100 μl DMEM and 20 μl CellTiter solution were added. The cells were incubated for 2 h before the formation of formazan was measured at 492 nm. The relative cell viability/activity of 1.00 corresponds to cells that have not received modified HEPES buffer. Significant difference (*$p < 0.01$) were found for 2.5 mM dithionite vs. the corresponding modified HEPES buffer [0 mM dithionite] at 90 and 120 min. Modified HEPES buffer without dithionite (open bar), and with 0.25 mM (light grey bar), 0.75 mM (dark grey bar) and with 2.5 mM dithionite (black bar).

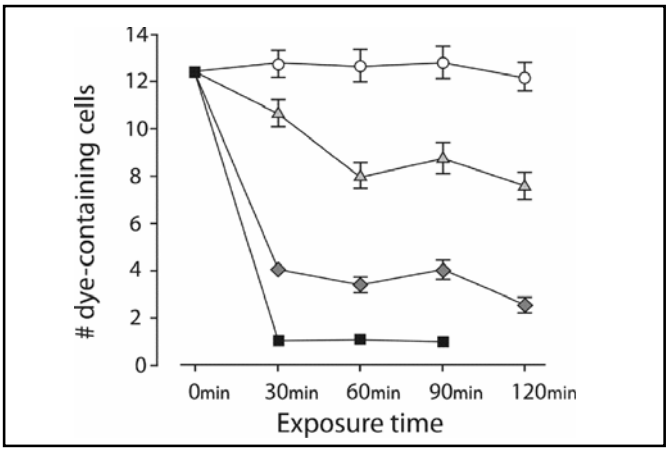

Fig. 3. Dithionite inhibits dye transfer in neonatal rat heart myofibroblasts. The control cells were in growth medium during the microinjections, and had not been exposed to modified HEPES buffer. The control cells had 12.71 ± 0.46 dye-containing cells per microinjection (mean ± SEM, n = 78 microinjections). All other points shown in the diagram are based on n = 42-58 microinjections. Significant difference ($p < 0.001$) were found for 0.75 mM and 2.5 mM dithionite at 30, 60, and 90 min, and for 0.25 mM at 120 min. Modified HEPES buffer without dithionite (open circle), and with 0.25 mM (grey triangle), 0.75 mM (grey diamond) and with 2.5 mM dithionite (filled square).

Statistical analysis

Data are expressed as mean ± SEM. Statistical differences in cell culture-studies were evaluated by using Mann-Whitney test or Kruskal-Wallis with Dunn's post-test. One-Way ANOVA

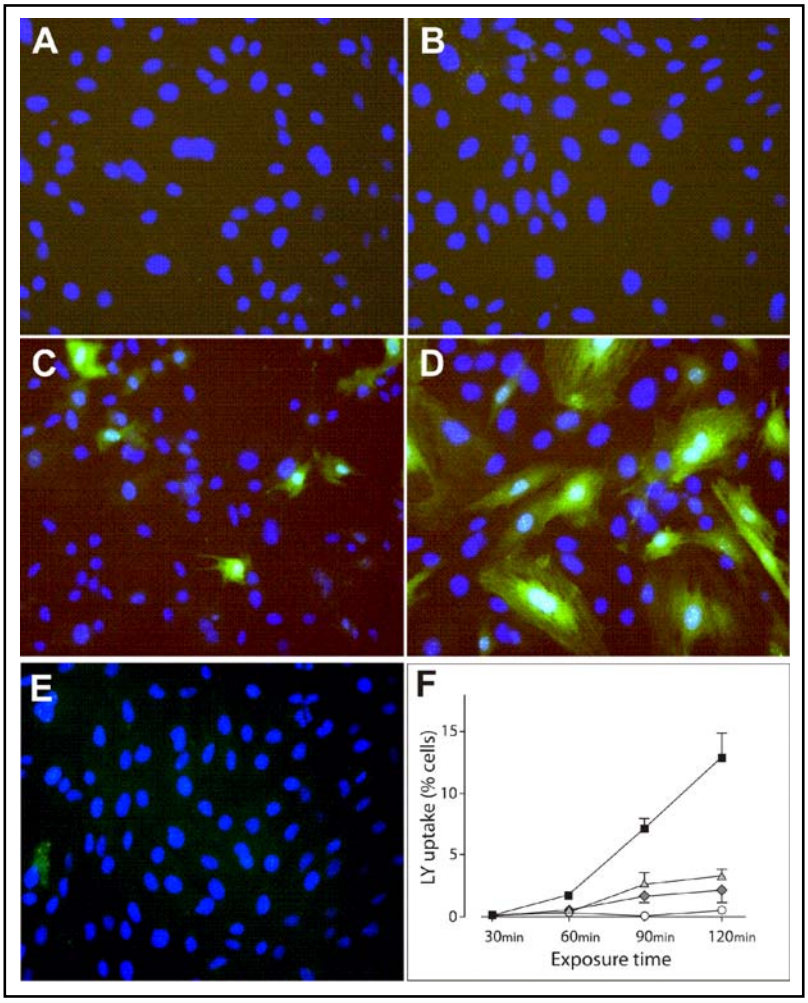

Fig. 4. Hemichannel opening in neonatal myofibroblasts induced by dithionite. Cells exposed to modified HEPES buffer and different concentrations of dithionite for 2 h before addition of Lucifer Yellow during the last 2 min of incubation. A) 0 mM dithionite, B) 0.25 mM dithionite, C) 0.75 mM dithionite, D) 2.5 mM dithionite, E) 2.5 mM dithionite for 2 h with 2 mM heptanol 10 min before addition of LY and F) LY uptake in percent of total cells with different concentration of dithionite over time. Modified HEPES buffer without dithionite (open circle), and with 0.25 mM (grey triangle), 0.75 mM (grey diamond) and with 2.5 mM dithionite (filled square). Significant differences were ($p < 0.01$) were found for 90 and 120 min exposures to 2.5 mM dithionite vs. modified HEPES buffer alone.

with Holm-Sidak post-test was used for comparing isolated perfused rat hearts. A value of $P<0.05$ was accepted as statistically significant.

Results

Cell viability in cell cultures

With respect to cell viability, up to 2 h exposure with modified HEPES buffer without dithionite did not affect the formation of the formazan product. A significant decrease was only observed after exposures to the highest concentration of dithionite (2.5 mM) and the longest exposure times (90 to 120 min) (Fig. 2). Dithionite is a scavenger of oxygen and it therefore rapidly decreases the oxygen tension in the solution [19, 21]. As shown in Fig. 1, 0.75 and 2.5 mM dithionite immediately removed all oxygen from the buffer, but already at 60 minutes, the oxygen tension was back at control level. Thus, the decrease in oxygen tension was transient, but significant cell death could be demonstrated.

Gap junction intercellular communication

When dye transfer was assessed by microinjection of Lucifer Yellow into single cells in a confluent monolayer cultured in growth medium, 12.71 ± 0.46 (mean ± SEM, n = 78 microinjections) dye-containing cells/microinjection were observed. This level of dye transfer was maintained during 2 h in the modified HEPES buffer without dithionite added (Fig. 3). Thus, the low pH and elevated potassium in the buffer did not affect dye transfer to any appreciable degree. The cells were exposed to 0.25, 0.75 or 2.5 mM dithionite for up to 2 h. The lowest concentration of dithionite had a moderate effect on dye transfer, inhibiting dye transfer by 30% at 1 to 2 h. The two highest concentrations of dithionite showed a pronounced inhibition of dye transfer at 30 minutes which were maintained throughout the exposure period. The results thus showed that the dithionite-induced decrease in dye transfer occurred before the reduction in cellular viability as measured by formazan generation. In this setting, it is therefore not reduced cell viability *per se* that caused decrease in dye transfer.

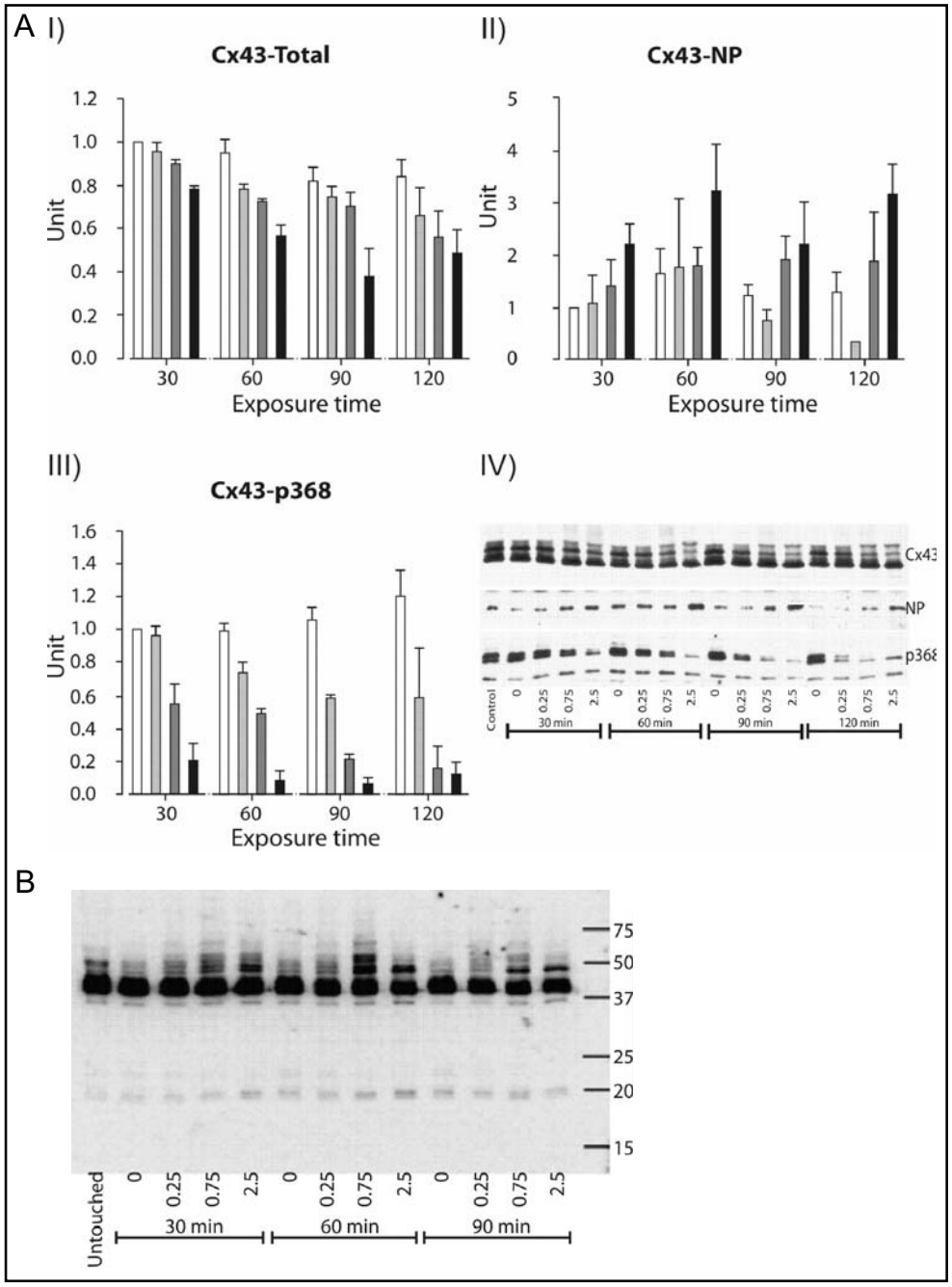

Fig. 5. A) Dithionite affects the phosphorylation status of Cx43. The cells were exposed to modified HEPES buffer and dithionite as indicated (0 mM to 2.5 mM dithionite). Modified HEPES buffer without dithionite (open bar) n=4, and with 0.25 mM (light grey bar) n=2, 0.75 mM (dark grey bar) n=4 and with 2.5 mM dithionite (black bar) n=4. Figure 4A I-IV shows densitometric quantification and results are normalised to 30 min modified HEPES buffer with 0 mM dithionite. I) Total Cx43 as detected by anti-Cx43 from Sigma, II) "Non-phosphorylated" Cx43 as detected by monoclonal antibody from Zymed, III) Phosphorylated Cx43 as detected by polyclonal phosphospecific anti-Cx43 antibody from Chemicon, IV) representative Western blots. The control cells were not exposed to modified HEPES buffer. Upper panel, anti-Cx43; second panel, anti-NP; and third panel, anti-pS368. Note the change in phosphorylation status of Cx43 as indicated by the three Cx43 antibodies. This is described in more detail in the text. Also note the shadow above Cx43, e.g. at 0.75 and 2.5 mM dithionite at 30 min exposure. B) Detection of potential degradation intermediates of Cx43. Acrylamide was increased to 12%, and 2x2 pixel binning and long exposure times were used to capture the images. The shadow above Cx43 can be resolved into several distinct bands. In addition, two shorter anti-Cx43 reactive bands were detected at around 23 and 20 kDa. Each of the two bands could be seen as a double band. Note that the 23 kDa band disappeared with increasing concentration of dithionite.

Hemichannels

We observed an increasing number of unsuccessful microinjections as a function of exposure time to, and concentration of, dithionite. We therefore asked whether this observation could have been caused by the opening of hemichannels. Consequently, we added LY to the modified HEPES buffer during the last two minutes of incubation, and quantified the number of LY-containing cells after fixation. Control cells incubated in modified HEPES buffer alone often had a large number of small vesicular structures, presumably early endosomes, labelled by LY during the 2 min incubation. This could easily be distinguished from the uniform uptake of LY into the whole cell (Fig. 4A-D). An increase in cells with a uniform labelling with LY was observed for cells exposed to dithionite, depending on time and concentration (Fig. 4A-D). Thus, hemichannels open upon exposure to high concentrations of dithionite, and this opening occurred in parallel with loss of cell viability. We have recently showed that pre-treatment with heptanol is cardioprotective

against ischemic injury and that heptanol increases time to mitochondrial permeability transmission pore opening [22]. By adding 2 mM heptanol 10 min before LY-exposure we prevented LY uptake into the cells (Fig. 4E). Also, Gap26 100 μM reduced the number of LY-containing cells by 67% and 85% in two separate experiments, while ^{10}Panx1 100 μM did not change the amount of LY-containing cells (data not shown). This result indicates that LY uptake into these cells is regulated and that this regulation probably is through Cx43 hemichannels.

Western blot

Modified HEPES buffer alone minimally affected Cx43 band pattern over a period of 2 h as detected by an antibody that recognizes all phosphorylated variants of Cx43 (Fig. 5A I). Cx43 showed two major bands, corresponding to P0 and P1, and a weaker band corresponding to P2. Two other anti-Cx43 antibodies, anti-NP and anti-pS368, both recognizing overlapping epitopes close to the C-terminal tail, were also used (Fig. 5A II, III). The former antibody mainly recognizes the nonphosphorylated version of Cx43, the latter antibody recognizes Cx43 when it is phosphorylated at S368. Thus, in case of any changes in the phosphorylation of the epitope, it would be expected that the two antibodies should show opposite responses. The exposure to 2.5 mM dithionite caused a pronounced decrease in the intensity of the P1 version of Cx43 already at 30 min. Concurrently, there was an increased recognition of Cx43 by the anti-NP antibody, and a clear decrease in recognition of Cx43 by anti-pS368. Only small changes were seen in the intensity of the P1 band (data not shown) when dithionite was added to serum-free medium. Thus, the combination of modified HEPES buffer and dithionite is needed for the effect, and some of the changes in phosphorylation are occurring in a serine-rich area close to the C-terminal tail of Cx43 as indicated by the opposite responses of anti-pS368 and anti-NP.

The amount of Cx43 appeared to decrease with increasing concentration of dithionite and increasing exposure time (Fig. 5A I). Ubiquitin- and proteasome-dependent degradation of Cx43 has received some attention [23-25] in addition to lysosomal degradation [26, 27], but also a more direct proteolytic action on Cx43 embedded into the plasma membrane or Golgi membrane is possible. This could be of importance, as experimental expression of the Cx43 C-terminal tail in cultured cells may have functional consequences (see Discussion). We therefore analyzed the samples using 12% polyacrylamide gels. Upon extended periods of image-capturing, and with

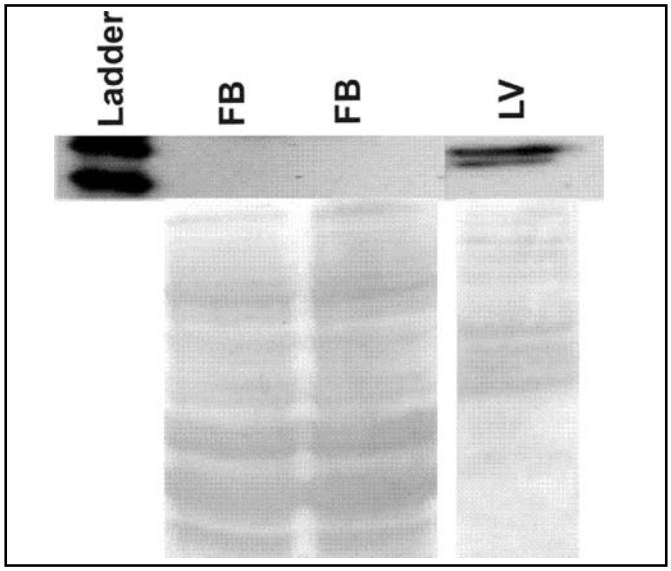

Fig. 6. Panx1 is expressed in heart left ventricle, but is not detected in neonatal rat heart myofibroblasts. Fig. 6 shows a representative blot with anti-Panx1 from Millipore. FB, neonatal rat heart myofibroblasts; LV, left ventricle from rat heart. Ladder, FB and LV are from the same gel. The corresponding Ponceau S-stained Western membrane is pasted below the blot to show that there are loaded higher amounts of protein in FB than in LV.

binning of pixels to increase the sensitivity, two fast-migrating double bands at 23 and 20 kDa were detected by anti-Cx43 (Fig. 5B). Densitometric quantification indicated that the 23 and 20 kDa bands constituted from 0.5% to a maximum of 2% of total amount of Cx43. The upper 23 kDa double band weakened upon exposure to dithionite, while there was a tendency for increased intensity of the lower band. Modified HEPES buffer alone minimally affected the two bands. Thus, dithionite appeared responsible for changing the relative amount of the two fast migrating bands.

The extended exposure time for the images also revealed a ladder-like pattern in the slow-migrating Cx43 versions visible as a shadow in Fig. 5A IV. The pattern could be due to ubiquitination. The modified HEPES buffer alone caused an apparent decrease in slow-migrating forms, which was reversed by the addition of dithionite. The highest amount of slow-migrating forms was seen at 60 min exposures to 0.75 or 2.5 mM dithionite.

Recent work in astrocytes has suggested that hemichannel opening in response to hypoxia could in fact be pannexins [12]. In order to exclude the possibility that Panx1 hemichannels were involved in the increased uptake of Lucifer Yellow under ischemic conditions we used Panx1 antibodies to test for the presence of Panx1

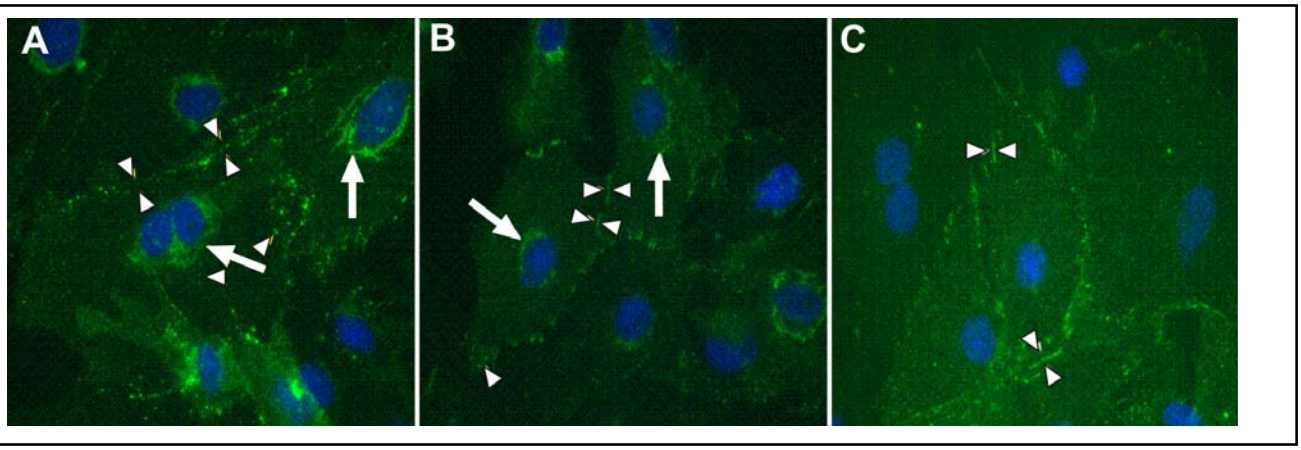

Fig. 7. A) Immunofluorescence of Cx43 in control neonatal myofibroblasts. The antibody recognizes all phosphovariants of Cx43. Note the well developed perinuclear staining (presumably in or close to the Golgi), the numerous small gap junction plaques at the cell-cell borders (apposing arrowheads), and vesicles in the cytoplasm (single arrowhead). The nuclei have been stained by DAPI. B) Immunofluorescence of Cx43 in neonatal myofibroblasts exposed to 0.75 mM dithionite for 90 min. The immunofluorescence staining of Cx43 has been enhanced in Photoshop. Note that most of the cells have relatively diffuse localization of Cx43 in the Golgi area (large arrows), and that gap junctions along the cell-cell borders often form longer structures (apposing arrowheads) than in control cells. Also some diffuse structures containing Cx43 are sometimes found close to the plasma membrane (single arrowhead). The nuclei have been stained by DAPI. C) Recognition of Cx43 by anti-NP in neonatal myofibroblasts exposed to 0.75 mM dithionite for 120 min. Note the major part of immunorecognition is located in or close to the plasma membranes, often in relatively long structures (apposing arrowheads), and with very little recognition in the perinuclear area. The nuclei have been stained by DAPI.

in protein extracts from neonatal myofibroblasts. Although the presence of Panx1 was confirmed in homogenates of rat heart tissue, no reactivity could be detected in the neonatal cardiac myofibroblasts (Fig. 6). The result suggests that neonatal rat heart myofibroblasts do not have Panx1 hemichannels, and this further supports the finding that [10]Panx1 did not affect LY-uptake through hemichannels.

Immunofluorescence

The neonatal cardiac fibroblasts showed relatively strong staining of Cx43 in Golgi-like structures in most cells, in addition to a number of relatively small spots located in or close to the cell membrane (Fig. 7A). Presumably, these spots are gap junction plaques. Many cells had numerous intracellular spots, presumably vesicles transporting Cx43 to the cell membrane, or internalized gap junctions destined for degradation. However, the growth pattern of these cells was quite unordered in that the cells showed extensive overlapping, which several times could make it difficult to clearly define spots as intracellular or not. Modified HEPES buffer alone caused a slight decrease in staining intensity of Cx43 in some cells over a period of 120 minutes, but this did not appear as a general effect. In contrast, the high concentrations of dithionite (2.5 mM) in modified HEPES buffer caused a decrease in staining intensity of Cx43 in most cells at 30 to 60 minutes of exposure.

As Western blots showed that the amount of Cx43 had decreased only slightly relative to unexposed control or cells exposed to modified HEPES buffer alone, these results may indicate a partial epitope masking. On the other hand, the low intensities of immunofluorescent staining of Cx43 at long exposure times (90 to 120 min) and high concentrations of dithionite (0.75 and 2.5 mM) are consistent with the decrease in amount of Cx43 in Western blots. Thus, the exposure to dithionite in modified HEPES buffer caused epitope masking, Cx43 degradation and an apparent redistribution of Cx43, depending on the concentration of dithionite and the exposure time (Fig. 7).

Triggered by the changes in Cx43 phosphorylation in Western blots detected by anti-pS368 and anti-NP, we also used these antibodies for immunofluorescent analysis of Cx43 localization. Anti-pS368 showed unexpectedly poor recognition with only a few spots in a few cells, even in unexposed control cells (not shown). The spots seemed to be located both along the cell-cell border and intracellularly. The low recognition of Cx43 even in unexposed control cells by anti-pS368 was surprising, as

a relatively strong band was found in Western blots (Fig. 5A). This might suggest epitope masking, either by the three-dimensional folding of Cx43 or by binding of other molecules to Cx43.

Consistent with the results obtained in Western blots, anti-NP showed poor recognition in unexposed control cells and in cells exposed to modified HEPES buffer alone. Only a low number of cells showed a few spots (not shown). After 90-120 min of exposure to 0.75 or 2.5 mM dithionite some cells showed a staining distributed along the membrane (Fig. 7C), sometimes in more or less diffuse aggregates close to the cell membrane or intracellularly, similar to the observation in cells analyzed by anti-Cx43 (Fig. 7B). Thus, this could suggest that at least a part of the Cx43 is dephosphorylated while present in the plasma membrane. Potentially, this could also be the signal for the redistribution from the small gap junction plaques seen in control cells (Fig. 7A) to the longer plaques seen in exposed cells (Figs. 7B and C).

Infarct size in perfused hearts

There were no statistically significant differences in ischemic risk zone volumes between the tree groups. Addition of Gap26 resulted in a significant reduction in infarct size compared to controls (infarct in % of risk zone volume 48.7±4.2% vs. 19.4±4.1%, $p<0.001$). Treatment with ^{10}Panx1 did not reduce infarct size compared to controls (48.7±4.2% vs. 52.6±5.7%, ns) (Fig. 8). There were no significant differences in coronary flow, heart rate and left ventricle developed pressure (LVDP) at baseline or at the end of the experiment between intervention groups and control.

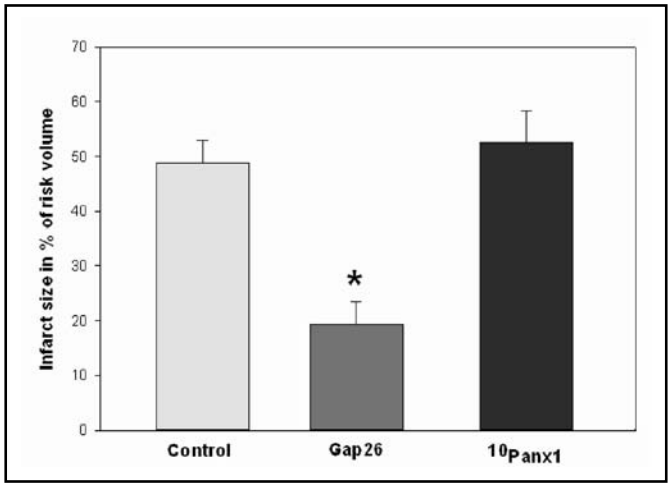

Fig. 8. Infarct size in isolated rat hearts expressed as percentage of ischemic risk volume. Control (light grey), Gap26, Cx43 mimetic peptide (dark grey), ^{10}Panx1, Pannexin1 mimetic peptide (black). *P<0.05, significant difference compared to control.

Discussion

In the present work, we used neonatal rat heart myofibroblasts to evaluate the effect of ischemia-like culture conditions (high potassium, low pH and reduced oxygen) on gap junctional communication between cells. The main findings were that ischemia-like conditions caused the gap junction channels to shut down the transfer of a dye to the neighbouring cells. In addition, Cx43 became partially dephosphorylated and the amount decreased. One possibility consistent with our data is that an ubiquitin-induced degradation of Cx43 takes place. Upon prolonged exposure to simulated ischemic conditions, hemichannels opened and cell death was apparent while the complete gap junctional channels remain closed. Consistent with Cx43 being the channel forming protein we could limit infarct size by preventing opening of Cx43-hemichannels at reperfusion after regional ischemia. Also, we were not able to detect the alternative hemichannel forming protein Panx1 in the cultured cells, and Panx1 hemichannel inhibitor did not change infarct size.

The simulated ischemia rapidly inhibited GJIC between neonatal rat myofibroblasts. Within the same timeframe changes could be seen with the two antibodies, anti-NP and anti-pS368. The two antibodies are said to detect the same epitope in nonphosphorylated and in phosphorylated form, respectively. As could be expected, the two latter antibodies showed opposite responses, and the loss of detection by anti-pS368 partly correlates with the loss of GJIC. Thus, the two phospho-sensitive antibodies more easily detect changes in phosphorylation of the relevant epitope of Cx43 than the antibody that recognizes all forms of Cx43. One reason for this is that several phosphorylation variants may have the same migration rate during SDS-PAGE. E.g., the Cx43 variants recognized by anti-NP and by anti-pS368 migrate at the same position [16, 28] (and data not shown). The reason for the change in phosphorylation of Cx43 could be the action of protein phosphatases, maybe in concert with Cx43 degradation and synthesis. It was previously shown that several of the major protein phosphatases could dephosphorylate Cx43 in a cell-free system [29] and PP2B has been implicated in cellular responses to hypoxia in the brain [30]. The present results strongly suggest that some of the dephosphorylations occur in the repetitive sequence (positions 364-373) close to the C-terminal tail of Cx43. This area may be of high importance for the

opening and the closing of the channels [31, 32]. Of special interest is that the suggested major protein kinase C phosphorylation site is S368, positioned in the middle of the repetitive sequence. Protein kinase C is involved in ischemic preconditioning effect in the heart [33], and previous results have shown that preconditioning delays the dephosphorylation in cardiac myocytes in culture [3]. Thus, dephosphorylation may occur because the balance of activity between phosphatases and protein kinase C has been displaced in favour of the phosphatases.

Simulated ischemia caused a decrease in Cx43 amount. Several mechanisms could be involved in the decrease of Cx43, including decreased translation and increased degradation. Both proteasomal and lysosomal degradation have previously been implicated in Cx43 turnover [23-27]. Although we have not studied this in more detail, the ladder pattern above the main Cx43 bands is consistent with ubiquitination. Some of the samples clearly indicated four slow migrating bands above the P1-P2 area. It was evident that dithionite added to modified HEPES increased the amount of the slow-migrating versions relative to modified HEPES buffer alone. At 2.5 mM dithionite and long exposure periods (60 min or more), the slow-migrating forms collapsed into one major slow-migration form, possibly containing only one ubiquitin. Ubiquitin-induced degradation of Cx43 might thus explain the decrease in the amount of Cx43 protein evident in Western blots after exposure to dithionite. In contrast to some previous studies [24, 34], ubiquitination appears to be induced by loss of phosphorylation and not by increased phosphorylation of Cx43. Our results do not give any information of the Cx43 isoform that becomes ubiquitinated, but with the low amounts of the P2 form, we believe it is likely that the NP or the P1 forms are the substrates for the conjugation. The role of protein ubiquitination, and more specifically Cx43 ubiquitination, in ischemic injury in the heart or in heart-derived cells is not clarified in detail. Recently Zhang et al [35] showed that preconditioning was associated with a marked reduction of ubiquitin-conjugated protein aggregation after cerebral ischemia in mice.

Anti-Cx43 detected a low amount of two fast-migrating (20 and 23 kDa) double bands in the Western samples. Recently, evidence was found for the presence of an approximately 20 kDa form of the C-terminal tail in several other systems [36, 37], and its presence was not due to accidental proteolytic activity during sample preparation [36]. Experimental expression of the C-terminal tail has revealed that this domain of Cx43 might have growth-regulatory properties independent of the channel functions of the intact protein [37-39]. However, in some contrast to the other groups [36, 37], we find two double band versions of the C-terminal tail. Each of the double bands is presumably due to variable phosphorylation. As the intact Cx43 may become ubiquitinated, the two fast-migrating variants could be due to the conjugation of one ubiquitin molecule to the C-terminal tail. However, we do not find this likely, as ubiquitin is around 8 kDa, and would probably have resulted in a larger difference in migration of the two variants. The other main possibility is that these are two cleavage variants of the C-terminal tail. Whether the presence of the free C-terminal tail in low amount in the cell has some biological functions remains to be seen, but it is intriguing that degradation of the 23 kDa form is induced by the ischemic buffer, while the 20 kDa form is not degraded. As the intensity of the 20 kDa form is increasing when the 23 kDa form disappears, it is possible that this is caused by an N-terminal cleavage of the 23 kDa form to generate the 20 kDa form. If the cleavage had been C-terminal, recognition by the anti-Cx43 antibody should have been lost.

The immunofluorescence experiments indicated some redistribution of Cx43 in the cells. The mechanism could be similar to acute Cx43 remodelling observed in the heart [3]. At the same time, epitope masking was observed. The two most likely explanations for epitope masking are other proteins binding to Cx43 covering the relevant epitope, or a spatial change in conformation that hides the epitope. The present experiments cannot distinguish between the two alternatives. It is tempting to speculate that there could be a connection between redistribution and epitope masking, e.g., by cytoskeletal proteins binding to Cx43 [40]. The cytoskeleton could also be responsible for the internalization of the gap junctions as annular junctions [41].

A remarkable, but not unique [5], observation is the opposing regulation of the complete channels and the hemichannels. Previous work has assumed the hemichannels simply are connexons not assembled into gap junction plaques, and Cx43 has been pointed out as a major source of hemichannels [1, 5, 42]. One of the arguments in favour of Cx43 hemichannels is that the hemichannel activity is sensitive to gap junction blockers [5]. However, this does not explain why other gap junction blocking situations, like ischemia, should have differential effects on complete channels and hemichannels. Only a few years ago, another family of gap junction proteins, the pannexins, was detected in mammals [43]. Later work has shown that pannexins have a strong propensity for

making hemichannels, and not complete channels [44, 45], although recent work may make the image more complex [46]. Furthermore, astrocytes exposed to hypoxia open hemichannels [5], and the pannexin hemichannels are sensitive to at least some of the agents that block connexin channels, like CO_2 [44] and carbenoxolone [43]. Although it has been largely assumed that these hemichannels consisted of Cx43, recent work has suggested that they could in fact be pannexins in astrocytes [12]. Western blot with two different antibodies was used to test whether Panx1 could be detected in neonatal rat heart fibroblasts. We were not able to demonstrate Panx1 expression or blockade of hemichannel opening in these cells. ^{10}Panx1, a Panx1 hemichannel blocker, did not have a cardioprotective effect. Therefore we conclude that both dye uptake after prolonged simulated ischemia and ischemia-reperfusion injury are due to opening of Cx43 hemichannels and not Panx1 hemichannels.

An important question that the present data cannot answer is if the observed effects in cell cultures are only due to the initial low oxygen tension in the medium or potential other parameters. The rapid inhibition of dye transfer might be due to the low oxygen tension, but the sustained low level of dye transfer is not, as the reversal of this response was much slower than the reversal of the oxygen tension. Low pH plus high potassium do not cause these effects. Dithionite is known to reduce ATP production [19], which may affect the kinase/phosphatase balance. Furthermore, dithionite has reducing capacity, and could affect e.g. disulfide bonds. Certain protein tyrosine phosphatases are redox sensitive which will have impact for the activity of the kinases that they control [47]. Alternatively, Cx43 itself might be the direct target for dithionite due the disulfide bridges in the extracellular loops, a conserved characteristic of the connexin family. Thus, multiple mechanisms could act together to give the observed effects. With the highest dose, 2.5 mM dithionite and 2 h of exposure, the dye injection experiments often failed. Although some cells showed morphological changes, possibly due to toxic effects, toxicity per se does not necessarily cause decreased GJIC [48]. We know that neonatal cardiac myofibroblasts also express connexin 45 (data not shown), and can not exclude that these channels may affect GJIC and hemichannel opening.

In conclusion, these data indicate that ischemia have opposite effects on hemichannels and functional gap junctional channels. Hemichannel opening occurs in parallel with reduction in cell viability, and by preventing opening of Cx43-hemichannels in the early ischemia-reperfusion period infarct size is reduced. A better understanding of the molecular mechanisms involved in hemichannel opening could help to develop a treatment that decreases the cellular injuries at reperfusion after ischemic attacks. Cx43-hemichannel opening plays an important role in the pathophysiology during early ischemia-reperfusion injury, and it is possible to reduce this injury by prevent opening of Cx43-hemichannels during early ischemia-reperfusion.

References

1 Saez JC, Retamal MA, Basilio D, Bukauskas FF, Bennett MV: Connexin-based gap junction hemichannels: gating mechanisms. Biochim Biophys Acta 2005;1711:215-224.

2 Jennings RB, Steenbergen C, Reimer KA: Myocardial ischemia and reperfusion. Monogr Pathol 1995;37:47-80.

3 Sundset R, Cooper M, Mikalsen SO, Ytrehus K: Ischemic preconditioning protects against gap junctional uncoupling in cardiac myofibroblasts. Cell Commun Adhes 2004;11:51-66.

4 Murry CE, Jennings RB, Reimer KA: Preconditioning with ischemia: a delay of lethal cell injury in ischemic myocardium. Circulation 1986;74:1124-1136.

5 Contreras JE, Sanchez HA, Eugenin EA, Speidel D, Theis M, Willecke K, Bukauskas FF, Bennett MV, Saez JC: Metabolic inhibition induces opening of unapposed connexin 43 gap junction hemichannels and reduces gap junctional communication in cortical astrocytes in culture. Proc Natl Acad Sci USA 2002;99:495-500.

6 Jain SK, Schuessler RB, Saffitz JE: Mechanisms of delayed electrical uncoupling induced by ischemic preconditioning. Circ Res 2003;92:1138-1144.

7 Ruiz-Meana M, Garcia-Dorado D, Lane S, Pina P, Inserte J, Mirabet M, Soler-Soler J: Persistence of gap junction communication during myocardial ischemia. Am J Physiol Heart Circ Physiol 2001;280:H2563-2571.

8 Noma A, Tsuboi N: Dependence of junctional conductance on proton, calcium and magnesium ions in cardiac paired cells of guinea-pig. J Physiol 1987;382:193-211.

9 Hawat G, Benderdour M, Rousseau G, Baroudi G: Connexin 43 mimetic peptide Gap26 confers protection to intact heart against myocardial ischemia injury. Pflugers Arch 2010;460:583-592.

10 Bruzzone R, Hormuzdi SG, Barbe MT, Herb A, Monyer H: Pannexins, a family of gap junction proteins expressed in brain. Proc Natl Acad Sci USA 2003;100:13644-13649.

11 Dahl G, Locovei S: Pannexin: to gap or not to gap, is that a question? IUBMB Life 2006;58:409-419.

12 Thompson RJ, Zhou N, MacVicar BA: Ischemia opens neuronal gap junction hemichannels. Science 2006;312:924-927.

13 Shestopalov VI, Panchin Y: Pannexins and gap junction protein diversity. Cell Mol Life Sci 2008;65:376-394.
14 Karpuk N, Burkovetskaya M, Fritz T, Angle A, Kielian T: Neuroinflammation leads to region-dependent alterations in astrocyte gap junction communication and hemichannel activity. J Neurosci 2011;31:414-425.
15 Nagy JI, Li WE, Roy C, Doble BW, Gilchrist JS, Kardami E, Hertzberg EL: Selective monoclonal antibody recognition and cellular localization of an unphosphorylated form of connexin43. Exp Cell Res 1997;236:127-136.
16 Cruciani V, Mikalsen SO: Stimulated phosphorylation of intracellular connexin43. Exp Cell Res 1999;251:285-298.
17 Cooper M, Ytrehus K: Cell survival signalling in heart derived myofibroblasts induced by preconditioning and bradykinin: the role of p38 MAP kinase. Mol Cell Biochem 2004;259:83-90.
18 Johansen D, Ytrehus K, Baxter GF: Exogenous hydrogen sulfide (H2S) protects against regional myocardial ischemia-reperfusion injury-Evidence for a role of K ATP channels. Basic Res Cardiol 2006;101:53-60.
19 Lambeth DO, Palmer G: Kinetics and Mechanism of Reduction of Electron-Transfer Proteins and Other Compounds of Biological Interest by Dithionite. J Biol Chem 1973;248:6095-6103.
20 Cheng Y, Gu XQ, Bednarczyk P, Wiedemann FR, Haddad GG, Siemen D: Hypoxia increases activity of the BK-channel in the inner mitochondrial membrane and reduces activity of the permeability transition pore. Cell Physiol Biochem 2008;22:127-136.
21 Lin Y, Liu A, Lu N, Li Y, Song Q, Yu H, Li X: Inhibitive effects of low oxygen and glucose deprivation on brain-pancreas relative protein expression via hypoxia- inducible factor-1 pathways. Cell Physiol Biochem 2008;22:353-362.
22 Johansen D, Sanden E, Hagve M, Chu X, Sundset R, Ytrehus K: Heptanol triggers cardioprotection via mitochondrial mechanisms and mitochondrial potassium channel opening in rat hearts. Acta Physiol (Oxf) 2011;201:435-444.
23 Laing JG, Beyer EC: The gap junction protein connexin43 is degraded via the ubiquitin proteasome pathway. J Biol Chem 1995;270:26399-26403.
24 Girao H, Pereira P: Phosphorylation of connexin 43 acts as a stimuli for proteasome-dependent degradation of the protein in lens epithelial cells. Mol Vis 2003;9:24-30.
25 Leithe E, Rivedal E: Epidermal growth factor regulates ubiquitination, internalization and proteasome-dependent degradation of connexin43. J Cell Sci 2004;117:1211-1220.
26 Laing JG, Tadros PN, Westphale EM, Beyer EC: Degradation of connexin43 gap junctions involves both the proteasome and the lysosome. Exp Cell Res 1997;236:482-492.
27 Qin H, Shao Q, Igdoura SA, Alaoui-Jamali MA, Laird DW: Lysosomal and proteasomal degradation play distinct roles in the life cycle of Cx43 in gap junctional intercellular communication-deficient and -competent breast tumor cells. J Biol Chem 2003;278:30005-30014.
28 Solan JL, Fry MD, TenBroek EM, Lampe PD: Connexin43 phosphorylation at S368 is acute during S and G2/M and in response to protein kinase C activation. J Cell Sci 2003;116:2203-2211.
29 Cruciani V, Kaalhus O, Mikalsen SO: Phosphatases involved in modulation of gap junctional intercellular communication and dephosphorylation of connexin43 in hamster fibroblasts: 2B or not 2B? Exp Cell Res 1999;252:449-463.
30 Li WE, Nagy JI: Connexin43 phosphorylation state and intercellular communication in cultured astrocytes following hypoxia and protein phosphatase inhibition. Eur J Neurosci 2000;12:2644-2650.
31 Lampe PD, TenBroek EM, Burt JM, Kurata WE, Johnson RG, Lau AF: Phosphorylation of connexin43 on serine368 by protein kinase C regulates gap junctional communication. J Cell Biol 2000;149:1503-1512.
32 TenBroek EM, Lampe PD, Solan JL, Reynhout JK, Johnson RG: Ser364 of connexin43 and the upregulation of gap junction assembly by cAMP. J Cell Biol 2001;155:1307-1318.
33 Ytrehus K, Liu Y, Downey JM: Preconditioning protects ischemic rabbit heart by protein kinase C activation. Am J Physiol 1994;266:H1145-1152.
34 Leithe E, Rivedal E: Ubiquitination and down-regulation of gap junction protein connexin-43 in response to 12-O-tetradecanoylphorbol 13-acetate treatment. J Biol Chem 2004;279:50089-50096.
35 Zhang HP, Yuan LB, Zhao RN, Tong L, Ma R, Dong HL, Xiong L: Isoflurane preconditioning induces neuroprotection by attenuating ubiquitin-conjugated protein aggregation in a mouse model of transient global cerebral ischemia. Anesth Analg 2010;111:506-514.
36 Joshi-Mukherjee R, Coombs W, Burrer C, de Mora IA, Delmar M, Taffet SM: Evidence for the presence of a free C-terminal fragment of cx43 in cultured cells. Cell Commun Adhes 2007;14:75-84.
37 Kardami E, Dang X, Iacobas DA, Nickel BE, Jeyaraman M, Srisakuldee W, Makazan J, Tanguy S, Spray DC: The role of connexins in controlling cell growth and gene expression. Prog Biophys Mol Biol 2007;94:245-264.
38 Moorby C, Patel M: Dual functions for connexins: Cx43 regulates growth independently of gap junction formation. Exp Cell Res 2001;271:238-248.
39 Dang X, Doble BW, Kardami E: The carboxy-tail of connexin-43 localizes to the nucleus and inhibits cell growth. Mol Cell Biochem 2003;242:35-38.
40 Giepmans BN: Gap junctions and connexin-interacting proteins. Cardiovasc Res 2004;62:233-245.
41 Leithe E, Brech A, Rivedal E: Endocytic processing of connexin43 gap junctions: a morphological study. Biochem J 2006;393:59-67.
42 Vergara L, Bao X, Cooper M, Bello-Reuss E, Reuss L: Gap-junctional hemichannels are activated by ATP depletion in human renal proximal tubule cells. J Membr Biol 2003;196:173-184.
43 Bruzzone R, Barbe MT, Jakob NJ, Monyer H: Pharmacological properties of homomeric and heteromeric pannexin hemichannels expressed in Xenopus oocytes. J Neurochem 2005;92:1033-1043.
44 Locovei S, Wang J, Dahl G: Activation of pannexin 1 channels by ATP through P2Y receptors and by cytoplasmic calcium. FEBS Lett 2006;580:239-244.
45 Zoidl G, Petrasch-Parwez E, Ray A, Meier C, Bunse S, Habbes HW, Dahl G, Dermietzel R: Localization of the pannexin1 protein at postsynaptic sites in the cerebral cortex and hippocampus. Neuroscience 2007;146:9-16.
46 Ishikawa M, Iwamoto T, Nakamura T, Doyle A, Fukumoto S, Yamada Y: Pannexin 3 functions as an ER Ca^{2+} channel, hemichannel, and gap junction to promote osteoblast differentiation. J Cell Biol 2011;193:1257-1274.
47 den Hertog J, Groen A, van der Wijk T: Redox regulation of protein-tyrosine phosphatases. Arch Biochem Biophys 2005;434:11-15.
48 Mikalsen SO: Heavy metal ions, cytotoxicity and gap junctional intercellular communication in Syrian hamster embryo cells. Altern Lab Anim (ATLA) 1992;20:213-217.